The THEMIS All-Sky Imaging Array - System Design and Initial Results from the Prototype Imager

Eric Donovan[1], Stephen Mende[2],
Brian Jackel[1], Harald Frey[2], Mikko Syrjäsuo[1], Igor Voronkov[1],
Trond Trondsen[1], Laura Peticolas[2], Vassilis Angelopoulos[2],
Stewart Harris[2], Mike Greffen[1], and Martin Connors[3].

Abstract THEMIS (Time History of Events and Macroscale Interactions During Substorms) is a NASA MIDEX mission scheduled for launch in 2006. THEMIS will consist of five magnetospheric satellites in equatorial orbits. Three of the spacecraft will have apogees around 12 Re, while the fourth and fifth will have apogees at ∼20 and ∼30 Re. The 12, 20, and 30 Re apogee orbits will have periods of 1, 2, and 4 sidereal days, respectively, meaning that all five spacecraft will be at or near apogee in the same meridian every four sidereal days. Furthermore, these conjunctions will always occur over central Canada throughout the mission duration. The five THEMIS satellites will be instrumented with particle and field detectors for measuring relevant plasma parameters, fields, and bulk velocities in the Central Plasma Sheet (CPS). The THEMIS constellation will bracket the Current Disruption (CD) and Near-Earth Neutral Line (NENL) regions and will provide for the first time an opportunity for unambiguous identification of the radial position in the CPS where the substorm process initiates. The primary scientific objective for THEMIS is to determine which of these processes is responsible for substorm onset. THEMIS cannot close this question without complementary ground-based observations in North America. To this end, THEMIS requires the deployment of twenty white light All-Sky Imagers (ASIs) in a continent-wide array. These ASIs will operate with a cadence of at least 1 image every five seconds, and will provide mission critical onset and early expansive phase information. In this paper, we present observations from the prototype THEMIS ASI for one substorm event. This image data demonstrates that the THEMIS ASI has the temporal and spatial resolution necessary to meet the mission requirements. Further, in this event we find that the growth phase arc shows wavelike azimuthal structuring and a brightening that occurs virtually simultaneously along the entire length of the arc that is within the ASI field of view. We attribute this wavelike structure to structure in the CPS. We anticipate that the THEMIS ASI array and *in situ* data will allow for the elucidation of the CPS process that generates this azimuthal structure.

1. Department of Physics and Astronomy, University of Calgary, Calgary, Canada, T2N 1N4.
2. Space Sciences Laboratory, University of California, Berkeley, 7 Gauss Way, Berkeley, CA 94720-7450
3. Athabasca University, 1 University Drive, Athabasca, Canada, T9S 3A3

1 Introduction

The phenomenological definition of the magnetospheric substorm is based on observations of auroral and magnetospheric processes [see e.g., *Akasofu*, 1977; *Rostoker*, 1999; *Voronkov et al.*, 2003]. The entire process involves a growth phase, breakup, and expansive and recovery phases[*Akasofu*, 1964; *McPherron*, 1970; *Rostoker et al.*, 1980]. During the growth phase, the auroral distribution moves equatorward, convection changes, and the magnetotail magnetic field topology becomes stretched. Immediately preceding the breakup, a pre-existing or newly formed auroral arc that is within the proton aurora intensifies [*Samson et al.*, 1992]. In the expansive phase, an expanding vortex reaches the auroral poleward boundary, which in turn also expands poleward [*Voronkov et al.*, 2003]. The expansive phase lasts tens of minutes, after which the system returns to a less disturbed state during the tens of minutes to hours that form the recovery phase.

The breakup (also "substorm onset") involves development of an arc into a vortex structure, poleward and zonal expansion of the vortex within the auroral oval, the dipolarization (i.e., relaxation) of the stretched magnetic field topology and concurrent Central Plasma Sheet (CPS) plasma energization, and enhanced ionospheric currents. As well as this auroral brightening, there are a host of other ionospheric and magnetospheric signatures that characterize the few minutes around onset. These include the negative H-bay and Pi2s, riometer absorption spikes, ELF/VLF wave activity, dispersionless and dispersed particle injections, and kink and sausage mode waves and reconnection in the mid-tail CPS [see e.g., *Akasofu*, 1964; *Olson*, 1999; *Spanswick et al.*, 2004; *Smith et al.*, 1996, 2002; *Baker et al.*, 1981, 1982; *Reeves et al.*, 1991; *Runov et al.*, 2003].

In Figure 1, we present summary observations of a substorm event that was described in detail by *Voronkov et al.* [2003]. During this event there was a small substorm (also called a *pseudobreakup* as described in *Koskinen et al.* [1993] and *Voronkov et al.* [2003]) at around 0400 UT and larger event at ∼0510 UT. In each case the growth phase exhibits equatorward motion of the optical aurora (as seen in the Meridian Scanning Photometer (MSP) keogram data in panel A). As well, the stretching of the magnetic field topology and its return to a more dipolar state is evident in the GOES 8 magnetic field direction (panel C). The negative H-bay (black curves, panel B) is most pronounced in the second event, as is the initial latitudinal localization of the enhanced ionospheric currents and their later expansion (red curves, panel B).

The substorm sequence highlighted in Figures 1 occurred over central Canada a few hours before local midnight. A picture of where in geomagnetic latitude and Magnetic Local Time (MLT) substorms usually occur has been pieced together on the basis of substorm observations over the last forty years. The statistics of substorm onset occurrence are illustrated nicely by the results of a comprehensive survey of auroral onsets seen in the NASA Imager for Magnetopause to Aurora Global Exploration (IMAGE) satellite Far-Ultraviolet (FUV) imager data that is described in the recent paper by *Frey et al.* [2004]. Their results indicate that onsets occur most frequently between 2200 MLT and local midnight, and between 60° and 70° degrees magnetic latitude. While the substorm is arguably a global process, typical substorms evolve out of a localized region in the pre-midnight sector ionosphere and magnetosphere.

A picture of the substorm as a dynamic sequence of energy storage and release in the magnetotail has evolved based primarily on phenomenological observations such as those highlighted in Figure 1. The growth phase is a period of energy storage in both the magnetotail magnetic field and CPS plasma. This energy is extracted from the solar wind through enhanced merging on the dayside. On the basis of statistical studies, it has been argued that the breakup is triggered by an interruption of this energy storage that results from, for example, a northward turning of the interplanetary magnetic field (IMF) [e.g. *Lyons et al.*, 1997]. The intensification, dipolarization, and enhanced ionospheric currents are all related to a diversion of magnetotail current through the ionosphere, and a release of energy stored in the stretched magnetic field topology. The current disruption begins as a localized disturbance and expands outwards from that onset location [see e.g., *Lui et al.*, 1992; *Ohtani et al.*, 1991; *Rostoker and Eastman*, 1987; *Wiens and Rostoker*, 1975; *Fairfield et al.*, 1999; *Frank et al.*, 2001, for examples of *in situ*, global auroral, and ground-magnetic views of this expansion process, respectively]. Initially, the diverted current forms a small "current wedge" connecting through the ionosphere that was first postulated by *Atkinson* [1967], and for which *McPherron* [1970] developed the phenomenological description that is now widely held to be correct.

The view of the substorm in terms of energy storage and release is still fundamentally phenomenological. Our objective in substorm studies is to elucidate the underlying plasma physical processes, one golden

example being the macroscale instability that leads to the onset. Existing observational capabilities do not provide a sufficient mix of spatial and temporal resolution and spatial coverage in both the ionosphere and the CPS to answer key substorm questions (such as, for example, what mid- or macro-scale instability leads to onset). For some aspects of the substorm problem this poses no great difficulty. The growth phase, for example, is well characterized by relatively low resolution data [*McPherron*, 1970; *Koskinen et al.*, 1993; *Voronkov et al.*, 1999]. The same can almost certainly be said for the recovery phase, though it has been less thoroughly studied [e.g., *Opgenoorth et al.,* 1994]. On the other hand, expansive phase onset is an extremely fast and apparently local process [see e.g., *Friedrich et al.*, 2001, and references therein] characterized both in the magnetosphere and the ionosphere by significant morphological changes that occur on time scales of tens of seconds or even less.

There are two well developed models of the substorm onset process. These are the Near Earth Neutral Line (NENL) [see e.g., *Hones*, 1979; *Baker et al.*, 1996], and Current Disruption (CD) models [see e.g., *Lui et al.*, 1992; *Lui*, 1996, 2001; *Ohtani et al.*, 1999]. Both are observationally based and incorporate auroral breakup at the equatorward edge of the auroral oval [*Akasofu*, 1977], current disruption in the inner magnetosphere (i.e., L=$\sim 5-10$), and mid-tail reconnection at ~20-30 R_E [*Hones*, 1984; *Lui*, 1996; *Baker et al.*, 1996]. The models differ in terms of the temporal sequence of events leading up to and through onset, where breakup maps to in the magnetosphere, where the mid-tail reconnection region maps to the ionosphere, and how these regions are physically coupled. For example, in the CD model inner plasma sheet current disruption and the associated dipolarization and auroral breakup occur first, initiate a rarefaction wave that propagates outwards which (in global substorms) causes reconnection in the mid-tail several minutes later. In the NENL model, mid-tail reconnection initiates rapid earthward flows, which brake several minutes later in the inner magnetosphere causing Pi2s, current disruption, auroral breakup, and other onset related effects. In short, the CD and NENL models differ in terms of the role played by and temporal sequence of mid-tail reconnection and current disruption.

Identifying and characterizing the sequence of events around substorm onset, with the goal of developing constraints for models of the involved physical processes, is one of the central objectives in space physics research. To this end, event studies have focussed on relatively rare serendipitous conjunctions of satellites and ground-based instrumentation [e.g. *Sergeev et al.*, 1995; *Pulkkinen et al.*, 1999; *Koskinen et al.*, 1993; *Nakamura et al.*, 1994; *Petrukovich et al.*, 1998; *Aikio et al.*, 1999; *Voronkov et al.*, 2003; *Kepko et al.*, 2004]. While these studies have advanced the state of knowledge, the fundamental question remains: **What physical process initiates substorm expansive phase onset**? The difficulty in resolving this question is a direct consequence of the lack of adequate high temporal and spatial resolution observations of onset phenomena with large enough ionospheric coverage and over a sufficiently large magnetospheric volume.

Resolution of this fundamental question requires a bold advancement in our observational capabilities. As stated above, the substorm onset is, by and large, an evening sector phenomenon. The CD and NENL regions are located near the inner edge of the plasma sheet (L $\simeq$6 to $\sim$ 10 Re) and in the midtail CPS (downtail distances of $\sim$ 20 to $\sim$ 30 Re), respectively [see e.g., *Baker et al.*, 1996; *Lui*, 1996]. The time for information to propagate from those two regions to the ionosphere or between these two regions is on the order of minutes. As seen in terms of its ionospheric disturbance, the substorm grows outwards from the initial breakup on a time scale of tens of minutes, ultimately covering many hours of local time [see e.g., *Jackel and Donovan*, 2002; *Liou et al.*, 2002]. In order to provide an observation-based resolution of the substorm onset question, simultaneous *in situ* observations must be obtained at locations inside of the CD region, between the CD and NENL regions, and tailward of the NENL region. Furthermore, additional observations are required in order to separate radial and azimuthal evolution and to ensure that the *in situ* observations are in the correct magnetic meridian. One can envisage two missions capable of providing such comprehensive magnetotail observations. A large number of satellites distributed throughout the CPS could provide a truly global picture of the substorm evolution in the magnetotail. In the short term, a more practical solution is to distribute a smaller number of satellites along one magnetic meridian, at radial distances bracketing the two regions of interest and to use ground-based observations to track the azimuthal evolution of the substorm.

The NASA THEMIS (Time History of Events and Macroscale Instabilities During Substorms) mission was conceived as a combined ground-based and satellite program specifically tailored to bring closure to this important question in space physics. THEMIS will consist of five satellites (referred to as P1 through P5 for "probe 1" through "probe 5") on highly elliptical equatorial orbits. All five will have an identical

complement of heritage particle, and electric and magnetic field instruments. Apogees of P5, P4, and P3 will be ∼12 Re, and of P2 and P1 will be ∼20 and ∼30 Re, respectively. The orbital periods will be 1 (P5, P4, and P3), 2 (P2), and 4 (P1) sidereal days. The satellites will be relatively phased along their orbits so that every four sidereal days there will be a conjunction wherein all five satellites are near apogee at around the same time. These conjunctions will effectively last for ten hours or more. As the conjunctions are separated by an integer number of sidereal days, every one will be over the same geographic region on the Earth for the duration of the mission. The conjunction meridian has been selected to maximize the impact of contemporaneous ground-based observations. In light of the fact that the largest readily accessible landmass under the auroral zone is in Canada, and Canada's long history of world-class ground-based space science observations, the conjunction meridian has been selected to be over central Canada.

The apogee conjunctions will occur every four sidereal days and the conjunction meridian will change in local time over the year. For example, three months after being at midnight, it will be at dusk. Since the conjunction meridian will always be over central Canada, it will be bracketed at all times by the geosynchronous NOAA GOES satellites (see Figure 2), which increases the number of satellites that will form the THEMIS constellation to 7. At conjunction, when the conjunction meridian is in the evening sector, this constellation will bracket (radially) the CD and NENL regions (again see Figure 2).

During substorm events, there will be ambiguity in the interpretation of the stand-alone satellite information due to the fact that the substorm disturbance expands azimuthally as well as radially in the CPS [see e.g., *Ohtani et al.*, 1991, 1992; *Liou et al.*, 2002]. To address this issue, the THEMIS program calls for 20 Ground-Based Observatories (GBOs) to be deployed across North America at auroral latitudes (see the map in Figure 3). Each GBO will house a white-light All-Sky Imager (ASI). GBOs that are more than ∼ 50km from ground-based magnetometers operated under the auspices of the Canadian GeoSpace Monitoring Program (CGSM; see cgsm.ca for links to the CANOPUS magnetometer array and the Natural Resources Canada CANMOS magnetometer array) will also house a University of California Los Angeles (UCLA) fluxgate magnetometer. The 20 GBOs, together with ground-based instruments operated by CGSM, Boston University, Ausberg College, the University of Alaska, Johns Hopkins University, UCLA, Stanford Research Institute, and other organizations will be used to track the ionospheric substorm ionospheric disturbance. Data from the ASIs will be used to identify the location and time of onset, and to track the evolution of the subsequent auroral disturbance [see e.g., *Lyons et al.*, 2002]. The magnetometers will be used to study the evolution of the ionospheric currents, and provide an rough estimate of the onset meridian (i.e., through careful analysis of the polarization of mid-latitude Pi2s) when auroral viewing conditions are poor [see e.g., *Nose et al.*, 1998; *Smith et al.*, 2002].

2 Instrumentation and Data

The formal scientific requirements that are to be met by the THEMIS ASI array are to determine the onset meridian to an accuracy of at least 1°, and onset time to an accuracy of better than 10 seconds. Although we shall return to the question of what constitutes onset, the spirit of these requirements is to be able to correctly identify the ionospheric location and timing of the first auroral brightening associated with the substorm expansive phase onset. More practical requirements are that development of the array be cost effective, that the instruments be reliable, and that a subset of the data be collected in real-time so that ongoing monitoring of instrument health is possible.

Consideration of the above requirements led to a solution that is a blend of off-the-shelf and purpose-built technologies. The THEMIS ground-support ASI is a non-intensified charge coupled device (CCD) based digital camera. Purpose built optics are mounted onto an off-the-shelf (panchromatic) Starlight Express MX716 low-light-level thermoelectrically cooled CCD camera. The custom made optical chain consists of a fish-eye objective, telecentric lens elements, and finally a relay lens to re-image the final image onto the MX716 8-mm diagonal Sony ICX249AL CCD sensor. This CCD has a quantum efficiency of 70% at 600 nm and utilizes the Sony-patented EXview HAD CCD technology, resulting in very good sensitivity. The camera is extensively used among astronomers.

The camera generates 752×580 pixel images. We will use on-chip 2×2 binning, capitalize on the fact that the image fits on a subframe of the CCD, and crop the image slightly. This results in a 256×256×16 bit image, giving a readout time of ∼1 second. We utilize an exposure time of 1 second. The 256 pixel wide

image provides spatial resolution of ∼1 km at zenith (assuming a 110 km emission altitude), and more than adequately meets our spatial resolution requirement. Together with compression of the image and some housekeeping activities, the total time needed to collect one image is slightly less than 2.5 seconds. Our plan at the present time is to collect one such image every five seconds, which satisfies our above mentioned temporal resolution requirement of onset identification to within ten seconds. Furthermore, each imager will operate identically, and imaging times will be simultaneous across the array (synched via GPS time). At the time of writing this paper, we are investigating the implications of increasing our cadence to 1 image every 3 seconds, and it is possible that we will implement that frame rate.

While the telecentric lens elements were designed to allow for the insertion of a "hot mirror" to protect the bare CCD from damage from sunlight during daytime imaging, we have since determined that exposure of the lenses and other elements of the optical chain to direct sunlight at high elevation angles can diminish the oveall instrument performance. Consequently, the team elected to install mechanical aluminum sunshades on each of the THEMIS ASIs. The sunshades are opened at the beginning of imaging on a particular day and closed at the end of imaging. They are controlled by a solenoid, and are designed to fail open rather than closed.

At a frame rate of one 256X256X16 bit image every five seconds, each imager will collect data at a rate of ∼1.5 MBytes per minute. We will operate the imagers whenever the sun is more than 12° below the horizon (i.e., nautical twilight). Given the distribution of geographic latitudes of the sites, which range from 49.4° (Kapuskasing, Ontario) to 68.3° (Inuvik, North West Territories), the average observing time per night, over all seasons and all stations, is 7.9 hours. This gives an average total of ∼0.75 GBytes per night and ∼270 GBytes/year/imager. With twenty imagers operating, the array will produce ∼5.5 TBytes of images per year. This corresponds to an array total of ∼40 million images per year.

In order to facilitate ongoing monitoring of instrument health and data quality, to maximize the impact of our education and public outreach program, to contribute to space weather programs, and to allow for the possibility of supporting observing campaigns, we view real-time data as a necessity. We further decided that we would use the newly implemented commercial satellite internet systems (TeleSat in Canada and Starband in Alaska) to recover the real-time data. Typical commercial packages allow us to recover data at a rate of only several GBytes per month from any given station, which corresponds to sustained uplink bandwidths of between 5 and 10 kbits per second. We are therefore only able to retrieve a subset of the images via the satellite internet connection. This subset will consist of roughly 720 8-bit pixel thumbnails per hour per imager, where the binning will be done "on the fly" in accordance with a set geomagnetic grid. These thumbnails will be merged into a mosaic and displayed in real time on the University of Calgary and University of California Berkeley THEMIS websites. The full resolution data will be stored on site on redundant hot-swappable external hard drives. Once or twice per year, the site custodian will ship one of the hot swappable drives to the University of Calgary, where the full resolution data will be integrated with the complete data set.

3 Coverage of the Ionospheric Region in Which Onsets Occur

From the outset, we chose locations for the THEMIS ground-based observatories with the understanding that onsets of substorms most often occur in the evening sector at typical auroral latitudes. As the program evolved, we have taken the time to quantify how well the planned imager array will provide coverage of the region in which substorm onsets occur.

This concern motivated the study of *Frey et al.* [2004], referred to in the introduction. A useful product of their study was the list of substorm onset times and locations that was published as ancillary digital information along with their paper. Using that list, it is straightforward to develop an analytical representation of the region within which substorm onsets occur most frequently, and hence to quantify how well the planned ASI array will provide coverage of that region. There are a number of ways that one might do this. Here, we chose to determine an elliptical region in a cartesian Magnetic Local Time (MLT) and magnetic latitude space within which a specified fraction of the IMAGE onsets (which we are assuming are representative of all onsets) occurred.

In the top panel of Figure 4, we have plotted the location of the *Frey et al.* [2004] onsets in MLT and magnetic latitude (using AACGM coordinates as described by *Baker and Wing* [1989]). We have overplotted

three contours which outline the regions within which 30, 50, and 70 per cent of the onsets occurred. The mission objective is to resolve the question of what causes substorm onset. The satellite constellation is designed to bracket the CD and NENL regions. Our "target" substorms are not going to be events that begin at anomalously low or high geomagnetic latitudes. For the purposes of this discussion, we focus our attention on the region contained within the the outer contour, within which 70% of substorm onsets occur.

Each day the ASI array will rotate under the substorm onset region. Assuming a 110 km emission height, we determined the fields of view of each imager, and converted their boundaries to geomagnetic coordinates. The bottom three panels in Figure 4 show the location of these fields of view at three universal times. In each case, a certain fraction of the onset region is within the merged fields of view. Figure 5 is a plot of the fractional coverage as a function of universal time. At 0000 UT, the eastern edge of the array rotates into the onset region, and 14 hours later the western edge crosses out of it. For roughly 8 hours every night, the imager fields of view cover roughly all of the onset region. For geographic reasons, the coverage is best when Western Canada is in the premidnight sector.

The onset region is roughly 4 hours wide in MLT. Thus, for roughly 2 months each year, the THEMIS constellation will be in the substorm onset local time sector. As the apogee conjunctions occur every four days, there will be roughly 15 nights per mission year-when the satellite constellation is ideally lined up to attack the primary mission objective. Statistics carried out with the CANOPUS magnetometer array indicate that, on average, there will be one substorm per night with an onset in the Canadian sector [*T. Hiebert, personal communication*]. The planned mission launch date will yield evening sector apogee alignments that occur during the winter months. We expect clear skies over any particular station at roughly 50% of the time, based on Canadian government meteorological statistics. Taken together, this information indicates that there we can expect roughly 10 events per mission year with an onset within the field of view of a THEMIS ASI, while the satellites are in apogee conjunction.

Of course, there will be alignments over the ASI array of P1 through P4 (i.e., all but the 30 Re apogee satellite) every two days, and of P1 through P3 every day. We can therefore expect the number of events for which we have *in situ* and good quality ASI data that can be used to study inner magnetospheric substorm processes to be approaching 40 per year.

4 An Example from the Prototype THEMIS ASI

A prototype of the THEMIS panchromatic ASI was deployed at the Athabasca University Geophysical Observatory in May 2003 (Athabasca is site 12 in Figure 3 and is at roughly 67.5° magnetic latitude). The objectives for deploying the prototype were to assist in the final stages of design of the ASI system, and to create a data set to ensure that the imager could adequately detect a typical substorm onset. As Athabasca is one of our lower geomagnetic latitude stations, we expected that the typical substorms would occur in the northern part of the imager field of view.

We have operated this imager on a nearly continuous basis since May 2003, and have built up a reasonable set of data that we have used in exploring binning to create thumbnails, in using stars to determine the imager orientation and optical characteristics, and to assure ourselves that this instrument will deliver on the THEMIS objectives. In this section we present one example substorm that had an onset captured in the Athabasca prototype imager. This event occurred to the north of Athabasca, and highlights some interesting science that we expect to explore with the THEMIS ASI array even prior to the launch of the satellites.

The event occurred around 0600 UT on October 4, 2003. At that universal time, Athabasca is located at an MLT of roughly 2200 hours. In Figure 6, we provide a four minute sequence of images each separated by five seconds. The first few images show the end stages of the growth phase, with a stable arc to the North of Athabasca. The CANOPUS meridian scanning photometer at Fort Smith (site 11 in Figure 3) also sees this arc, although it is to the south of Fort Smith. Although care must be taken in the interpretation of the Fort Smith data, the arc as seen in the oxygen green line emissions appears to be located at roughly 66° magnetic latitude), which is just inside the poleward edge of the ASI field of view (again, see Figure 3). This is consistent with the location of the onset arc, which can be seen near the treeline in the images.

There is now ample evidence that the poleward border of the evening sector oxygen red line emissions is co-located with the separatrix between open and closed magnetic field lines [*Blanchard et al.*, 1995]. Poleward motion of the separatrix during the expansive phase is an indication of magnetic reconnection at

the boundary between open and closed magnetic field lines. While the viewing conditions over Fort Smith and Gillam (Site 13 in Figure 3) are not optimal, the CANOPUS meridian scanning photometers at both those sites produced Oxygen red line (630 nm) data from which we can infer some information about whether or not this event is a pseudobreakup or a breakup developing into full onset involving lobe flux reconnection monitored both on the Fort Smith and Gillam meridians.

The arc begins to brighten at or after 061930 UT (in hhmmss format). Figure 7 is a stack plot of data from a number of ground-based instruments for 12 minutes that span this onset. In the top two plots, we show the X-component of the magnetic field (top) and the single beam riometer voltage, both from Fort Smith. The X-component simply shows a negative H-bay. Furthermore, magnetic field data from stations along the east-west CANOPUS chain that includes Fort Smith shows that the onset was more or less simultaneous at Fort Simpson and Fort Smith (sites 8 and 11 in Figure 3), and expanded rapidly to sites to the west and east of that pair over the subsequent few minutes. The riometer shows a spike in radio wave absorption that peaks near 0621 UT. This absorption spike satisfies a criterion that has recently been developed for the identification of substorm injections that are likely dispersionless [*Spanswick et al.*, 2005]. There is no such absorption feature at any site west or east of Fort Smith, but there is one several minutes later at Fort McMurray, which is between Athabasca and Fort Smith.

The third panel from the top shows mid-latitude and sub-auroral Pi2 activity clearly visible in the unfiltered magnetic eastward components from three Natural Resources Canada stations that essentially span the continent. These were Victoria (green - on the West Coast), Meanook (black - about 30 kilometers from Athabasca), and Ottawa (red - east of the Great Lakes). Not shown are the magnetic field measurements from the geosynchronous GOES satellites. GOES 10, roughly one hour MLT west of Fort Smith (roughly conjugate to Fort Simpson), registered a dipolarization at around 0621 UT. At GOES 12, more than three hours in local time east of Fort Smith, there was no identifiable signature of this onset. There was a dispersed ion and electron injection, the latter with several secondary "echoes", evident in the LANL 1994-084 satellite SOPA particle fluxes. The dispersed ion injection arrives after 0620 UT at the spacecraft, which was located at roughly 1600 MLT. The dispersed electron injection arrives later than that, as would be expected for an onset at or around 0620 UT.

The bottom three panels in Figure 7 are summaries of data from the Athabasca THEMIS prototype ASI. The integrated brightness (third from bottom) was obtained by simply summing the data in the partial images in Figure 6. There is a sudden increase in brightness beginning at 061925 (in hhmmss format) or 061930 UT (there is arguably some uncertainty at the five second level but not at the ten second level). The integrated brightness increases rapidly from that point, showing virtually pure linear growth (i.e., $\propto e^{\gamma t}$) remarkably similar to that shown by the red line growth phase arc discussed in *Voronkov et al.* [2003] (see their Figure 6). This linear growth occurs during 15 subsequent images starting with the image at 061925 UT. In a breakup sequence that shares many similarities with the event discussed by *Voronkov et al.* [2003], the initial linear increase in brightness lasts only a few minutes, stalls, and starts up again several minutes later. The process is decidedly a two-step one.

The second panel from the bottom is a traditional keogram, showing the equatorward drifting growth phase arc that brightens, and expands poleward. The bottom panel is a less conventional *ewogram* (for "east-west-o-gram") which has been produced as follows. The ewogram vertical axis corresponds to the east-west direction, with west corresponding to the bottom of the panel and east the top. The color indicates *integrated column brightness* (note that this is different than the typical keogram where brightness along a line is plotted). As we are using a rectangular portion of the CCD, there are the same number of pixels summed for each column. In some columns we are including an unimaged portion of the CCD, and hence our results might be skewed. In the ewogram the increase in brightness shows up as a rapid brightening of the growth phase arc along its entire east-west extent (i.e., extending at least out to the limits of the imager field of view). This shows up as a vertical band just to the right of the vertical dashed line. The arc brightens over several images. At 061950 the arc brightens dramatically in one region along its length (see the corresponding image in Figure 6 for confirmation of this). There is rapid expansion westward (down) and less rapid expansion eastward of this disturbance. The secondary brightening which begins at roughly 062330 UT shows up remarkably clearly on the ewogram and does not expand out to the edge of the imager field of view.

Figure 8 is a stack plot of column integrated brightnesses for the images taken between 061820 and 061940 UT. In this plot, we have taken only 100 columns from the ewogram data. Each curve is a plot of

brightness along the arc, with west to the right and east to the left. The plots are offset so that the absolute brightness cannot be inferred from the plot (it can be inferred from the ewogram in Figure 7). The times corresponding to each curve are given on the right side of the plot. The red curve is data from the image corresponding to the dashed vertical line in Figure 7. Thus, these curves are from images leading up to the beginning of the first brightening. At least in this instance, the arc shows pronounced structuring along its length (i.e., in the east-west direction) that is wavelike in character. The amplitude of the periodicity in brightness gets larger right before the sudden increase in overall brightness. The wave appears to be more or less stationary, and the east-west wavelength is roughly 50 km. This corresponds to an azimuthal wavelength of ∼800 km in the equatorial plane of the magnetosphere.

Based on the information presented here we suggest the following. The meridian scanning photometer red line data shows that this event is a fully developed substorm rather than a pseudobreakup. Data from the CANOPUS east-west chain of magnetometers and riometers show that the onset was near the Fort Smith meridian which is also the Athabasca meridian (i.e., where the prototype imager is located). The riometer data further shows that there was a dispersionless injection associated with this onset also on the Fort Smith meridian. The dispersionless injection, and the dipolarization seen at GOES occur almost simultaneously with the auroral brightening seen in the THEMIS prototype ASI. The auroral brightening is preceded by the development of azimuthal (i.e., east-west) structuring of the brightness of the growth phase arc. That structure is wavelike, but not propagating along the arc. The auroral brightening begins in an azimuthally limited region along the arc and expands rapidly westward and less rapidly eastward.

5 Discussion

In this paper, we have presented a description of the THEMIS MIDEX program along with its primary scientific motivation which is to close the question of what physical process causes substorm expansive phase onset. We described the motivation behind the THEMIS ASI array, and our plans for its implementation. We demonstrated that the ASI array will provide essentially complete coverage of the MLT and magnetic latitude region within which most substorm onsets occur for at least 8 hours every day. Based on statistics of substorm onset, and estimates of average cloud cover, we predict roughly ten events per year with an optical onset within one of the ASI fields of view during good viewing conditions, and during one of the THEMIS apogee conjunctions. This also means we will have as many as 40 events with an onset observed by one of the imagers and a conjunction involving P1, P2, and P3 (i.e., the three satellites with one day orbits).

The THEMIS ASI array will produce roughly 40 million images per year. In this paper, we have not addressed the significant difficulties associated with managing an image data set of this type. At the present time, we are developing tools for producing keograms and ewograms, merging images into mosaics, and cloud detection. We are also establishing protocols for useful metadata, as well as exploring the use of a relational database to manage the image data set. A particularly interesting information science research direction has emerged out of auroral imaging programs in recent years. In recent work by *Syrjasuo et al.* [2002] and *Syrjasuo and Donovan* [2004], computer vision algorithms are being developed for automatic classification of auroral images. Our intention is that these techniques will greatly increase the usefulness of the THEMIS ASI data set for auroral science, over and above its designed use in substorm studies.

Based on the event presented in Section 4, we are certain that the THEMIS panchromatic ASIs will be able to detect the optical brightening corresponding to onset with a temporal accuracy of at least ten seconds. We point out, however, that the objectives of the THEMIS mission demand much more of the ASI data than simply identifying a feature called "onset". It is much more important that we develop an understanding of what magnetospheric processes correspond to specific changes in the aurora. In other words, in order to maximize the synergy between THEMIS, the THEMIS Ground-based Observatory program, and other ground-based programs, it is absolutely essential to understand the physical and causal linkages between the ionospheric and *in situ* observations. Questions such as "what is the ionospheric signature of mid-tail reconnection?", "what is the ionospheric signature of a flux rope?", and "what magnetospheric physical process corresponds to the sudden brightening of the aurora?" must be resolved if THEMIS is to achieve its stated objectives.

The ASI data presented in Section 4 is a tantalizing taste of what is to come. The development of azimuthal structure in the brightness of the growth phase arc just prior to the optical brightening is particularly

interesting. The data in Figures 7 and 8 indicate that the auroral arc brightens across a distance that spans the ASI field of view in only seconds. This brightening is followed almost immediately by a dispersionless injection in the same meridian. Recent work by *Spanswick et al.* [2005] suggests that the dispersionless injection starts out as an azimuthally extended radially limited disturbance in the geosynchronous region (or just outside of it). This suggests that the sudden brightening and azimuthal structuring of the arc is related to the instability responsible for destabilizing the cross-tail current in the inner magnetosphere. It will be very interesting to explore this azimuthal evolution of the growth phase arc right at the time of optical brightening using data from several ASIs spread out in the east-west direction (for example, White Horse, Fort Simpson, and Fort Smith).

High resolution THEMIS ASI data has provided additional evidence to a previously suggested scenario for the near-Earth onset, and also proved sufficient for meeting the mission scientific requirements. Significantly improved time resolution clearly shows the multi-stage character of onset, as earlier suggested by Voronkov et al., [2003] on the basis of 30 sec MSP data analysis. This includes linearly unstable growth of arc-aligned wave structure, its saturation and further development into vortical structure which expands poleward preceding full onset (as indicated by disruption of the poleward boundary of auroral red line emissions). The initial arc uniform brightness growth and near-monochromatic wave length of its perturbation suggest that onset starts with an azimuthally stretched non-dispersive structure such as current and/or flow shear, associated with the arc. Supportive multi-instrument magnetic and optical observations confirms correct spatial and temporal position of the observed features. Based on the ground observations, it appears that this sample event was internally triggered and developed into full onset. However, we are not asserting that this is the only, or even a common, onset scenario. More importantly, signatures of mid-tail processes in ground-based data are not well understood. Comprehensive resolution of the connection between magnetospheric events and ionospheric signatures, as well as the question of where and how onset begins are central THEMIS tasks.

The THEMIS GBO program, and in particular the ASI part of that program, presents us with a unique opportunity. We will create an auroral image data set with a better combination of spatial coverage (continental scale and comparable to that achieved by the FREJA UV Imager) and temporal (the baseline requirements call for one image every 5 seconds) and spatial (i.e., 1 km or less at zenith) resolution than has ever been available before. The ASI data will have stand-alone value for studies of the aurora, and provide important observations complementing those of other geospace missions, with SWARM being an excellent example. The ASI data will provide a never before seen high time resolution picture of the evolution of the substorm disturbance across several hours of local time, with exciting implications for studies of ballooning, bursty-bulk flows, and other large-scale magnetotail instabilities. Together with the satellite, and other ground-based data, the ASI images will contribute to significant advancements in our understanding of the substorm process. Finally, the ASI data set will be visually stunning, and a powerful tool for education and public outreach.

Acknowledgements The THEMIS ASI array program is supported by the grant NASA RTOP NM710832 and the Canadian Space Agency via the THEMIS-C Phase 0 contract. Funding from the Canadian Natural Sciences and Engineering Research Council supported work leading up to the start of CSA funding. E. Donovan is grateful to the coIs of the University of Calgary Institute for Space Research Major Facilities Access grant for providing the Canadian THEMIS team access to that NSERC funding. Mikko Syrjäsuo is financially supported by Alberta Ingenuity.

References

Aikio, A. T., V. A. Sergeev, M. A. Shukhtina, L. I. Vagina, V. Angelopoulos, W. Baumjohann, and G. D. Reeves, Characteristics of pseudobreakups and substorms observed in the ionosphere, at the geosynchronous orbit, and in the tail, *J. Geophys. Res.*, *104*, 12,263, 1999.

Akasofu, S.-I., The development of the auroral substorm, *Planet. Space Sci.*, *12*, 273–282, 1964.

Akasofu, S.-I., *Physics of Magnetospheric Substorms*, D. Reidel, Dordrecht, 1977.

Atkinson, G., Polar magnetic substorms, *J. Geophys. Res.*, *72*, 1491, 1967.

Baker, D., P. Stauning, E. H. Jr., P. Higbie, and R. Belian, Near-equatorial, high resolution measurements of electron precipitation at $l \simeq 6.6$, *J. Geophys. Res.*, *86*, 2295, 1981.

Baker, D., E. H. Jr., R. Belian, P. Higbie, R. Lepping, and P. Stauning, Multiple-spacecraft and correlated riometer study of magnetospheric substorm phenomena, *J. Geophys. Res.*, *87*, 6121, 1982.

Baker, D., T. Pulkkinen, V. Angelopoulos, W. Baumjohann, and R. McPherron, The neutral line model of substorms: Past results and present view, *J. Geophys. Res.*, *101*, 12,975–13,010, 1996.

Baker, K., and S. Wing, A new magnetic coordinate system for conjugate studies at high latitudes, *J. Geophys. Res.*, *94*, 9139, 1989.

Blanchard, G. T., L. R. Lyons, J. C. Samson, and F. J. Rich, Locating the polar cap boundary from observations of 6300 å auroral emission, *J. Geophys. Res.*, *100*, 7855, 1995.

Fairfield, D., et al., Earthward flow bursts in the inner magnetotail and their relation to auroral brightening, akr intensifications, geosynchronous particle injections and magnetic activity, *J. Geophys. Res.*, *104*, 355, 1999.

Frank, L. A., J. B. Sigwarth, W. R. Paterson, and S. Kokubun, Two encounters of the substorm onset region with the geotail spacecraft, *J. Geophys. Res.*, *106*, 5811, 2001.

Frey, H. U., S. B. Mende, V. Angelopoulos, and E. F. Donovan, Substorm observations by image-fuv, *J. Geophys. Res.*, p. doi:10.1029/2004JA010607, 2004.

Friedrich, E., J. C. Samson, I. Voronkov, and G. Rostoker, Dynamics of the substorm expansive phase, *J. Geophys. Res.*, *106*, 13,145, 2001.

Hones, E. W., Transsient phenomena in the magnetotail and their relation to substorms, *Space Sci. Rev*, *23*, 393–410, 1979.

Hones, E. W. (Ed.), *Magnetic reconnection in space and laboratory plamas*, AGU, 1984.

Jackel, B., and E. Donovan, Azimuthal substorm propagation inferred from an l-shell chain of ground-based magnetometers, *Proceedings of the Sixth International Conference on Substorms*, p. 129, 2002.

Kepko, L., M. G. Kivelson, R. L. McPherron, and H. E. Spence, Relative timing of substorm onset phenomena, *J. Geophys. Res.*, *109*, doi:10.1029/2003JA010,285, 2004.

Koskinen, H., R. Lopez, R. Pellinen, T. Pulkkinen, D. Baker, and T. Bösinger, Pseudobreakup and substorm growth phase in the ionosphere and magnetosphere, *J. Geophys. Res.*, *98*, 5801–5813, 1993.

Liou, K., C.-I. Meng, A. T. Y. Lui, P. T. Newelll, and S. Wing, Magnetic dipolarization with substorm onset, *J. Geophys. Res.*, *107*, doi:10.1029/2001JA000,179, 2002.

Lui, A., Current disruption in the earth's magnetosphere: Observations and models, *J. Geophys. Res.*, *101*, 13,067, 1996.

Lui, A., Current controversies in magnetospheric physics, *Rev. Geophys.*, *29*, 535, 2001.

Lui, A., et al., Current disruption in the near-earth neutral sheet region, *J. Geophys. Res.*, *97*, 1461, 1992.

Lyons, L., G. Blanchard, J. Samson, R. Lepping, T. Yamamoto, and T. Moretto, Coordinated observations demonstrating external substorm triggering, *J. Geophys. Res.*, *102*, 27,039–27,051, 1997.

Lyons, L., I. Voronkov, E. Donovan, and E. Zesta, Relation of substorm breakup arc to other growth-phase auroral arcs, *J. Geophys. Res.*, *107*, DOI:10.1029/2002JA009,317, 2002.

McPherron, R., Growth phase of magnetospheric substorms, *J. Geophys. Res.*, *75*, 5592–5599, 1970.

Nakamura, R., D. Baker, T. Yamamoto, R. D. Belian, E. A. B. III, J. R. Benbrook, and J. R. Theall, Particle and field signatures during pseudobreakup and major expansion onset, *J. Geophys. Res.*, *99*, 207, 1994.

Nose, M., T. Iyemori, M. Takeda, T. Kamei, D. Milling, D. Orr, H. Singer, E. Worthington, and N. Sumitomo, Automated detection of pi2 pulsations using wavelet analysis: 1. method and an application for substorm monitoring, *Earth, Planets, and Space*, *50*, 773, 1998.

Ohtani, S., K. Takahashi, L. Zanetti, T. Potemra, R. McEntire, and T. Iijima, Tail current disruption in the geosynchronous region, *AGU Monograph on Substorms*, p. 131, 1991.

Ohtani, S., S. Kokubun, and C. Russell, Radial expansion of the tail curent disruption during substorms: a new approach to the substorm onset region, *J. Geophys. Res.*, *97*, 3129, 1992.

Ohtani, S., F. Creutzberg, T. Mukai, H. Singer, A. Lui, M. Nakamura, P. Prikyl, K. Yumoto, and G. Rostoker, Substorm onset timing: the december 31, 1995 event, *J. Geophys. Res.*, *104*, 22,713–22,727, 1999.

Olson, J., Pi2 pulsations and substorm onsets: A review, *J. Geophys. Res.*, *104*, 17,499, 1999.

Petrukovich, A., et al., Two spacecraft observations of a reconnection pulse during an auroral breakup, *J. Geophys. Res.*, *103*, 47, 1998.

Pulkkinen, T., et al., Spatial extent and dynamics of a thin current sheet during the substorm growth phase on december 10, 1996, *J. Geophys. Res.*, *104*, 28,475, 1999.

Reeves, G., R. D. Belian, and T. A. Fritz, Numerical tracing of energetic particle drifts in a model magnetosphere, *J. Geophys. Res.*, *96*, 13,99714,008, 1991.

Rostoker, G., The evolving concept of a magnetospheric substorm, *J. Geophys. Res.*, *61*, 85, 1999.

Rostoker, G., and T. E. Eastman, A boundary layer model for magnetospheric substorms, *J. Geophys. Res.*, *92*, 12,187, 1987.

Rostoker, G., S.-I. Akasofu, J. Foster, R. A. Greenwald, Y. Kamide, K. Kawasaki, A. T. Y. Lui, R. L. McPherron, and C. T. Russell, Magnetospheric substormsdefinition and signatures, *J. Geophys. Res.*, *85*, 1663, 1980.

Runov, A., et al., Current sheet flapping motion and structure observed by cluster, *Geophys. Res. Lett.*, *30*, doi:10.1029/2002GL016,730, 2003.

Samson, J., L. Lyons, P. Newell, F. Creutzberg, and B. Xu, Proton aurora and substorm intensifications, *Geophys. Res. Lett.*, *19*, 2167–2170, 1992.

Sergeev, V. A., V. Angelopoulos, D. G. Mitchell, and C. T. Russell, In situ observations of magnetotail reconnection prior to the onset of a small substorm, *J. Geophys. Res.*, *100*, 19,121, 1995.

Smith, A., M. Freeman, and G. Reeves, Postmidnight vlf chorus events, a substorm signature observed at the ground near l=4, *J. Geophys. Res.*, *101*, 24,64124,654, 1996.

Smith, A. J., M. Freeman, S. Hunter, and D. K. Milling, Vlf, magnetic bay, and pi2 substorm signatures at auroral midlatitude ground stations, *J. Geophys. Res.*, *107*, doi:10.1029/ 2002JA009,389, 2002.

Spanswick, E., E. Donovan, W. Liu, D. wallis, A. Aasnes, T. Hiebert, B. Jackel, and M. Henderson, Substorm associated spikes in high energy precipitation, *AGU Monograph on Physics of the Inner Magnetosphere (in press)*, 2004.

Spanswick, E., E. Donovan, and R. Friedel, Ground-based detection of dispersionless injections, *GRL*, *submitted*, 2005.

Syrjasuo, M., and E. F. Donovan, Diurnal auroral occurrence statistics obtained via machine vision, *Ann. Geophys.*, *22*, 1103, 2004.

Syrjasuo, M., E. F. Donovan, and M. Peura, Using attribute trees to analyse auroral appearance over canada, *Proc. of IEEE Workshop on Applications of Computer Vision*, 2002.

Voronkov, I., E. Friedrich, and J. C. Samson, Dynamics of the substorm growth phase as observed using canopus and superdarn instruments, *J. Geophys. Res.*, *104*, 28,491, 1999.

Voronkov, I., E. Donovan, and J. Samson, Observations of the phases of the substorm, *J. Geophys. Res.*, *108*, 1073, 2003.

Wiens, R. G., and G. Rostoker, Characteristics of the development of the westward electrojet during the expansin phase of magentospheric substorms, *J. Geophys. Res.*, *80*, 2109–2128, 1975.

Figures and Captions

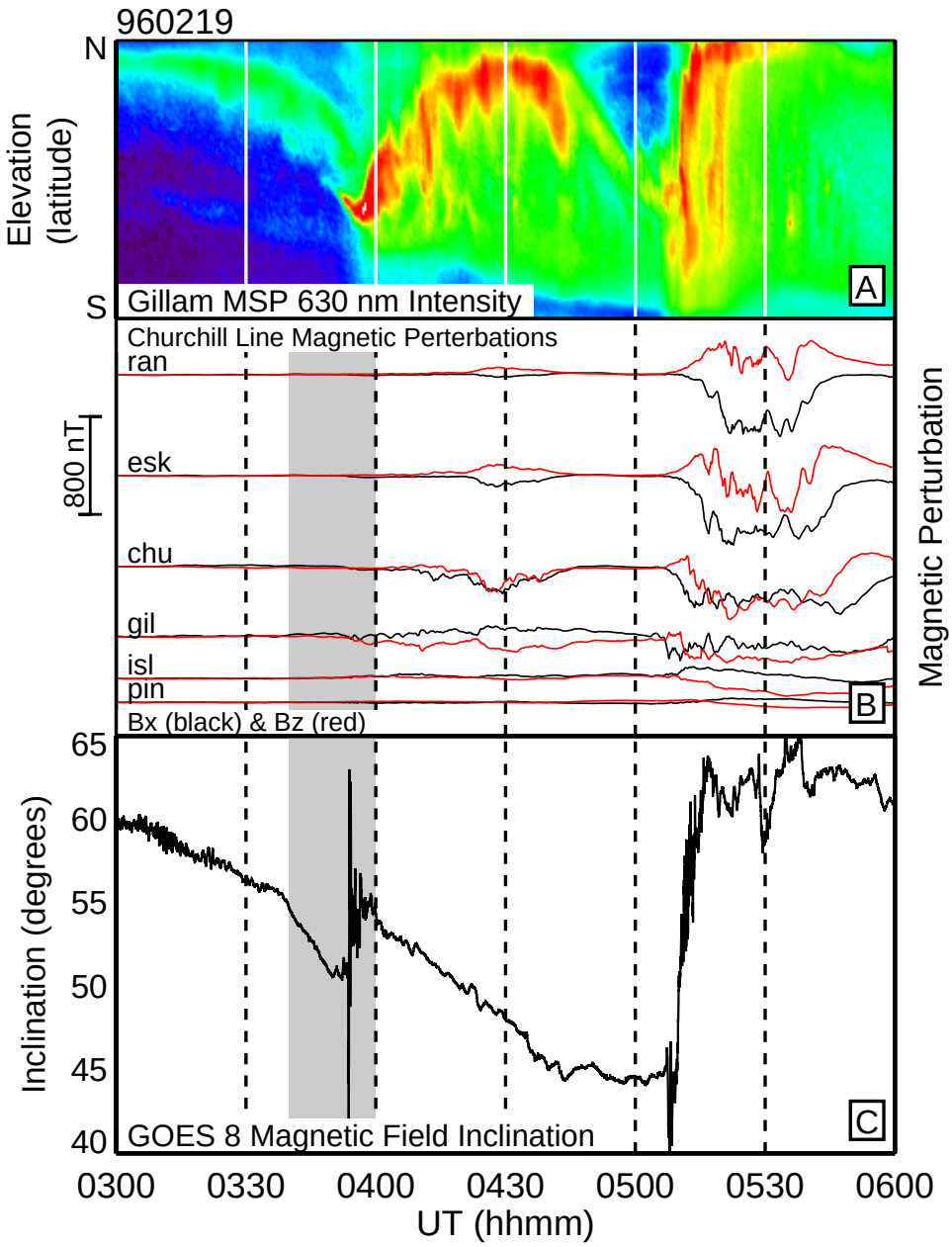

Figure 1: Sequence of pseudobreakup followed by full onset observed over central Canada on February 19, 1996. **A:** Keogram of 630 nm intensity from the CANOPUS Gillam MSP. The vertical axis corresponds to elevation, with north at the top and south at the bottom. The first ionospheric signature of the pseudobreakup (~0350 UT) is the brightening of a thin arc at the equatorward edge of the diffuse low energy electron aurora. **B:** Ground magnetic northward (X) and vertical (Z) perturbations along the CANOPUS Churchill line. Note the small enhancement of the electrojet during the pseudobreakup and the major enhancement during the breakup. The X-deviations and onset show the classic development of the current wedge. **C:** Magnetic inclination at GOES 8 (just above the magnetic equator, magnetically conjugate to the East coast of Hudson Bay) showing small dipolarization and major dipolarization during the pseudobreakup and onset, respectively.

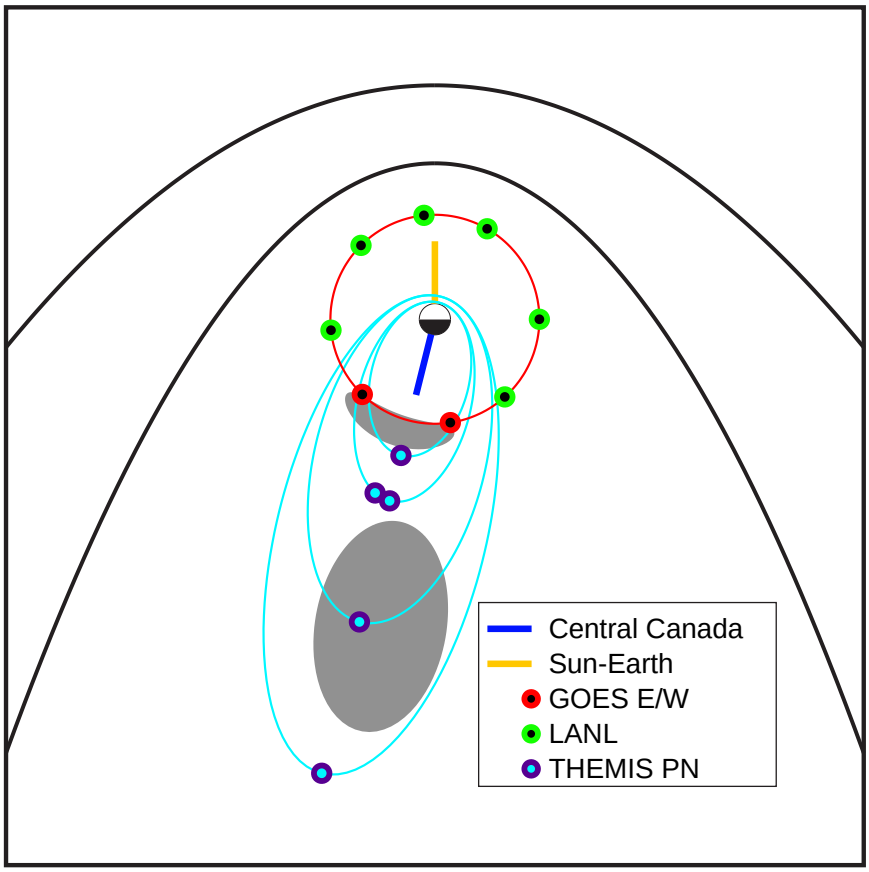

Figure 2: Locations of the five THEMIS and two GOES satellites during an apogee conjunction in the evening sector. Reasonable locations for the Current Disruption (CD) and Near-Earth Neutral Line (NENL) regions are indicated by the grey shading, the CD region being the closer of the two to the Earth. The substorm evolution in the CPS is both azimuthal and radial. This will introduce ambiguity in the interpretation of the *in situ* THEMIS data. One motivation for the ground-based component of THEMIS is to follow the azimuthal evolution of the disturbance as projected into the ionosphere. Subject to mapping limitations, this will allow the placement of the conjunction meridian relative to the onset meridian.

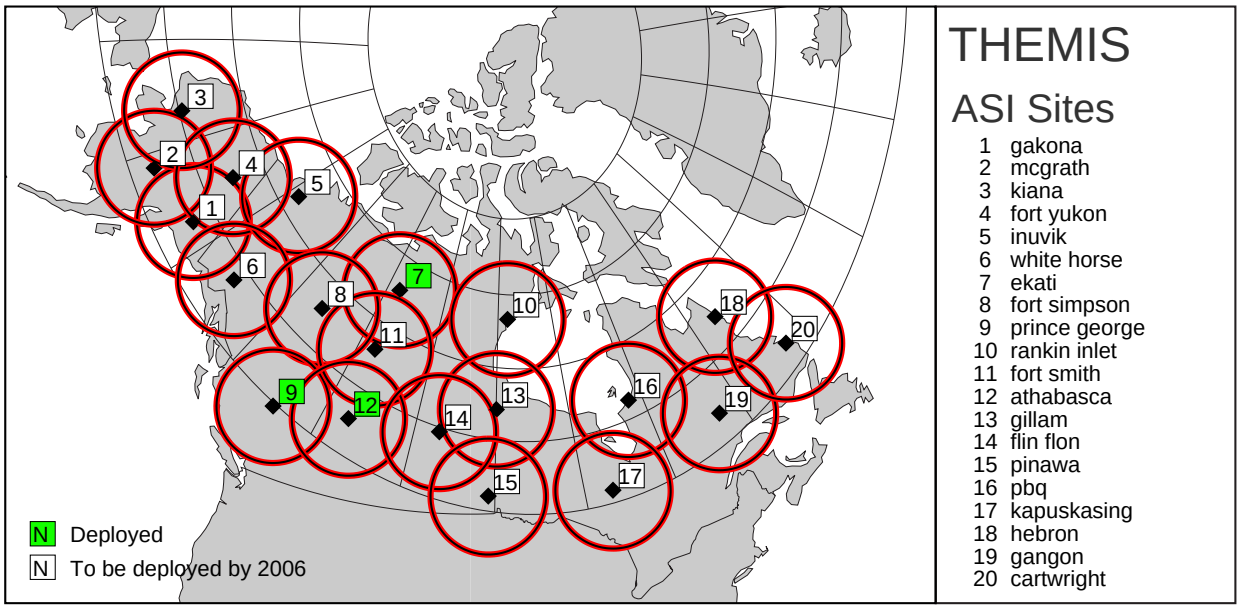

Figure 3: THEMIS ASI fields of view (at 110 km).

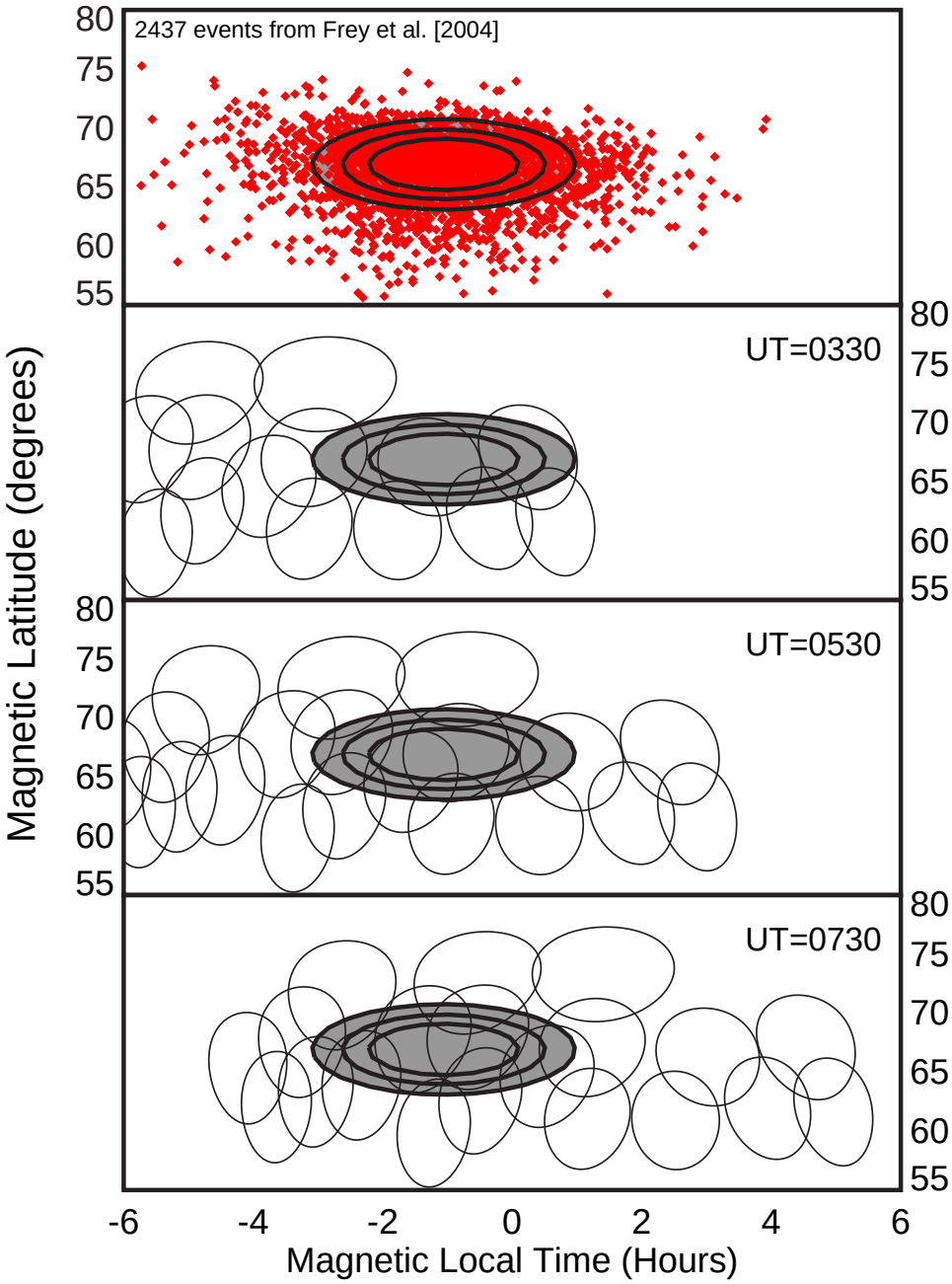

Figure 4: The top panel shows the locations of the onsets from *Frey et al.* [2004] from which we determined the substorm onset region within which 70% of substorm onsets occur. The oval with major and minor axis roughly 4 MLT hours and 8° of magnetic latitude, respectively, encloses a region in magnetic coordinates within which 70% of substorm auroral breakups occur (the two smaller ovals enclose 50% and 30% of onsets). The bottom three panels show the onset region overplotted on the fields of view of the THEMIS ASI array, assuming 110 kilometer emission height, for three different universal times.

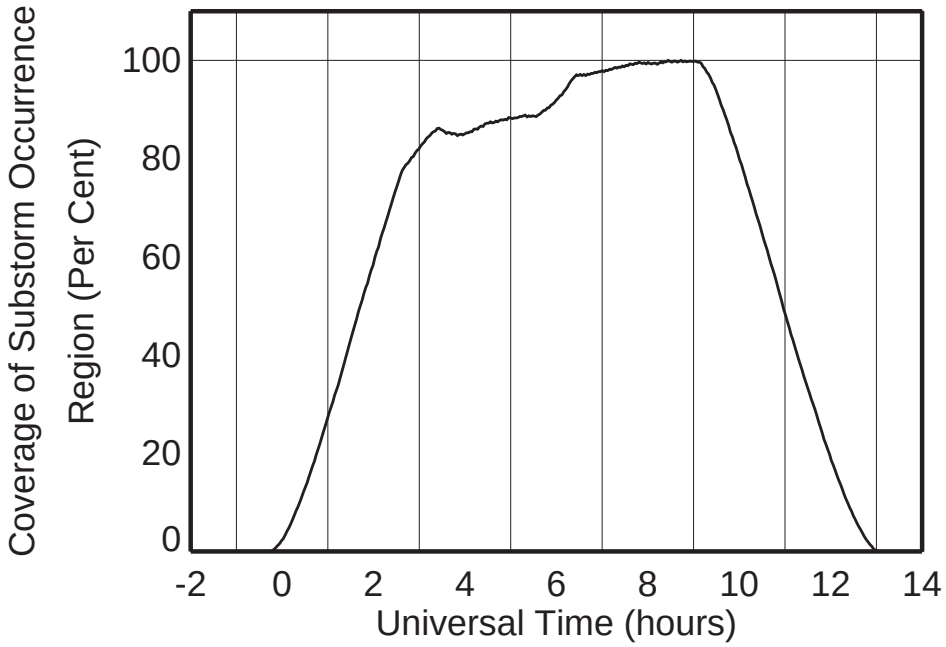

Figure 5: Over the course of the night, the THEMIS array slides across the substorm onset region, and the fractional coverage of that region varies. This plot shows the fractional coverage of the substorm onset region by the THEMIS ASI array (i.e., the 70% oval) as a function of UT.

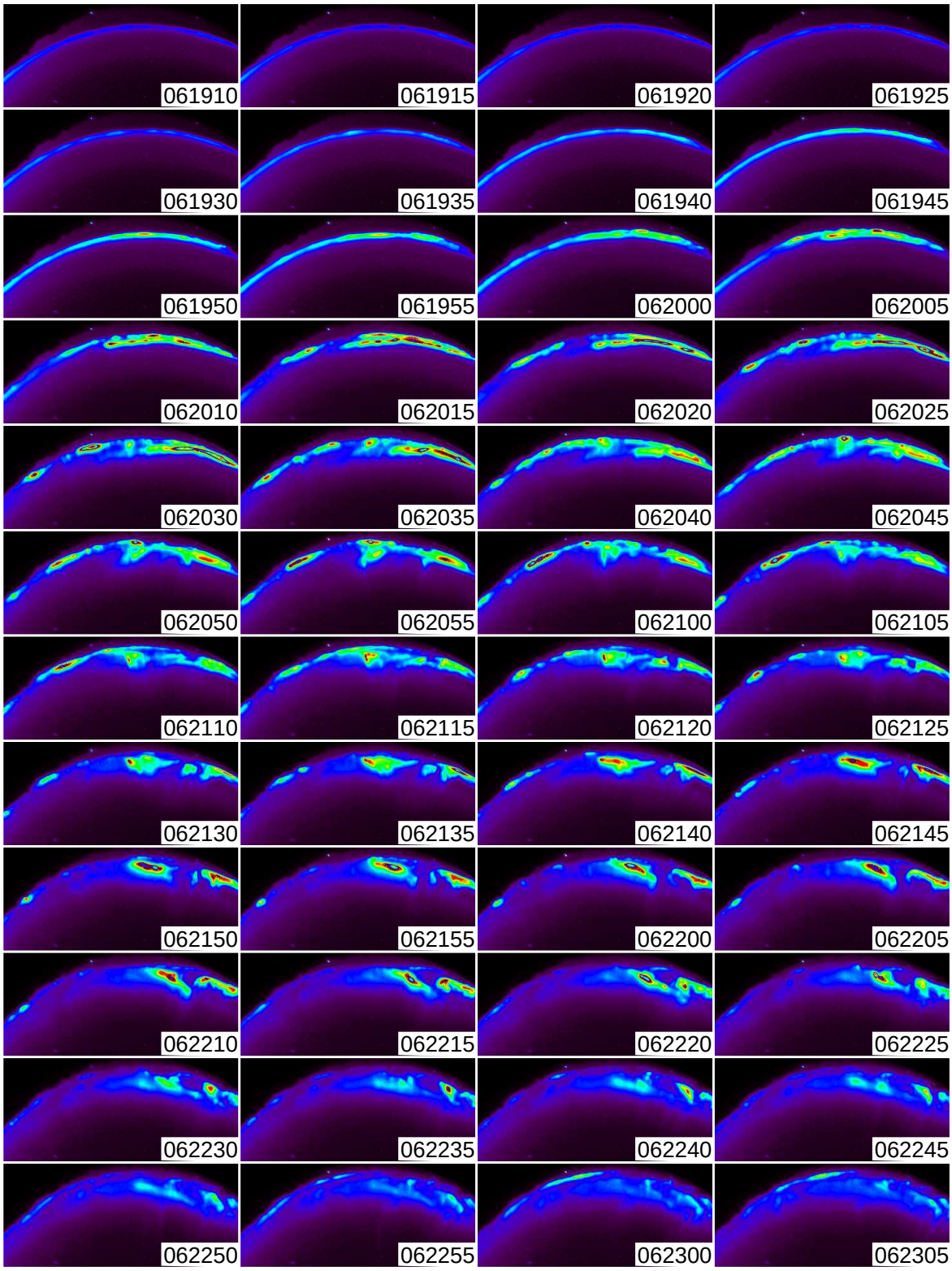

Figure 6: Sequence of partial images from the THEMIS prototype at Athabasca. These partial images are from the north of Athabasca, over Fort Smith, and show the very late growth phase and expansive phase of a small substorm. The numbers in the corner of each partial image indicate the time (hhmmss) at which the image was obtained. The event is examined in more detail in Figure 7.

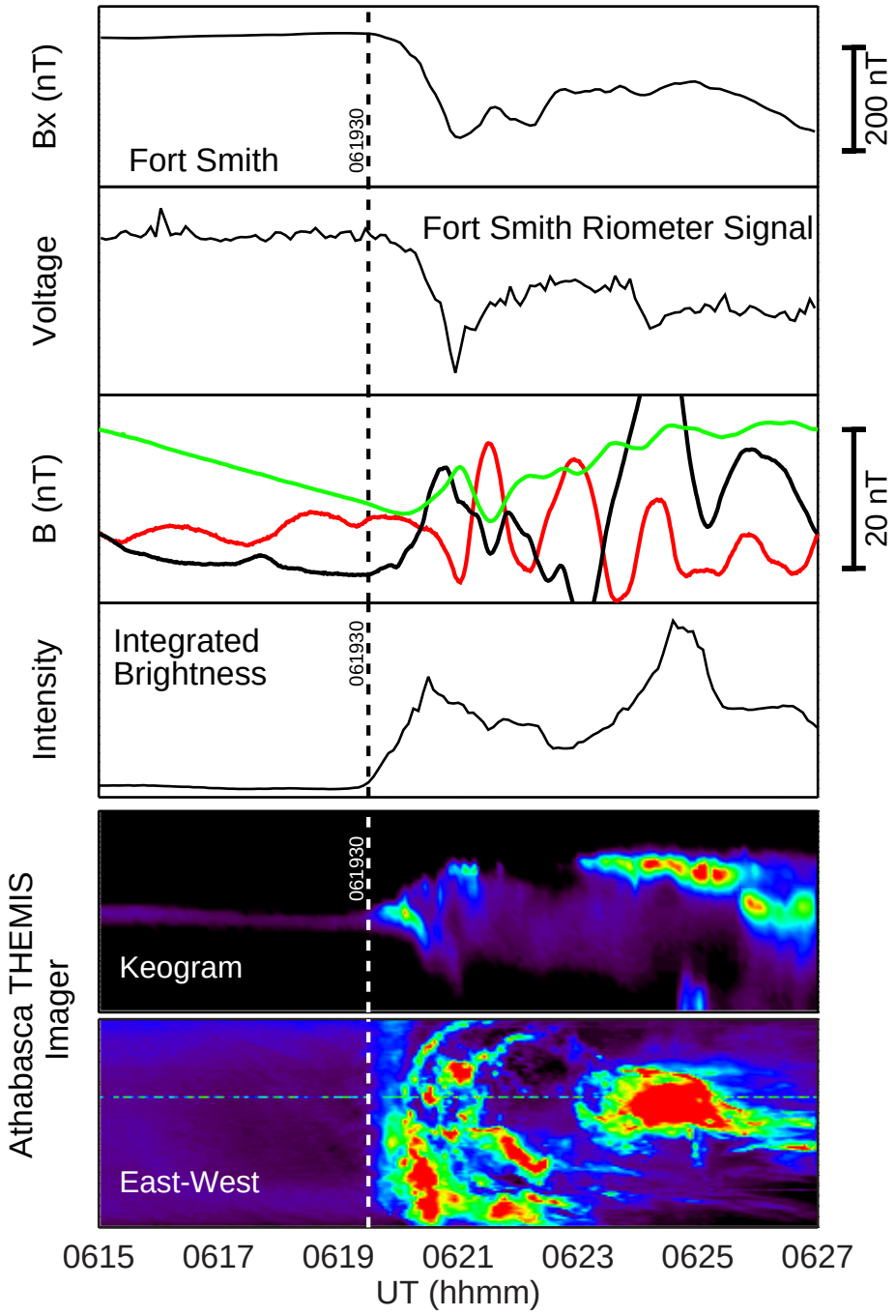

Figure 7: Stack plot of ground-based magnetometer, riometer, and ASI data from the minutes around the substorm onset shown in Figure 6. The onset is north of Athabasca. The top panel shows the negative H-bay (Fort Smith), and the second panel enhanced riometer absorption. Mid-latitude (green and red) and high latitude (black) Pi2s are shown in the third panel. The fourth panel shows the integrated brightness in the images shown in Figure 6. The bottom two panels are North-South and East-West keograms, again created from the images shown in Figure 6. The vertical dashed line indicates the start of the auroral brightening.

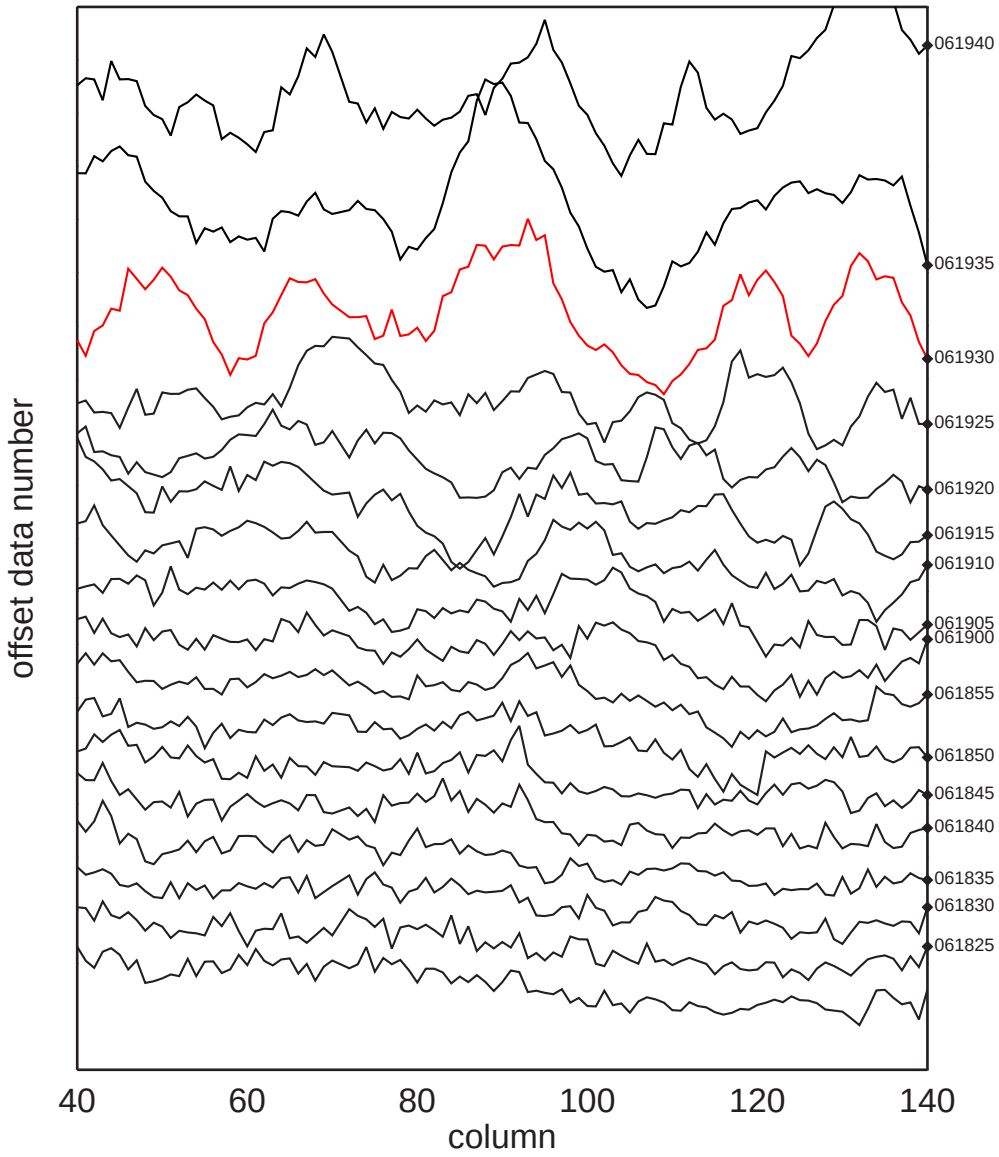

Figure 8: Stack plot of integrated column brightnesses from the sequence of images leading up to the auroral brightening. The red curve is from the image taken at the time indicated by the vertical dashed line in Figure 7